International Conference on Applied Energy 2020
Dec. 1 - Dec. 10, 2020, Bangkok / Virtual
Paper ID: 0394

Online State of Charge Estimation of Liquid Metal Battery using Dual Adaptive Extended Kalman Filter

Cheng Xu, E Zhang, Kai Jiang, Kangli Wang*

State Key Laboratory of Advanced Electromagnetic Engineering and Technology, School of Electrical and Electronic Engineering, Huazhong University of Science and Technology, Wuhan, Hubei, China 430074.

ABSTRACT

Accurate state of charge (SOC) estimation is an important evaluation index for battery management system. However, the SOC estimation accuracy is influenced by many factors, in which aging is one of the most important factors. Therefore, real-time parameter identification is necessary for accurate SOC estimation. In this paper, we proposed a dual adaptive extended Kalman filter algorithm for the SOC and parameter co-estimation of liquid metal battery, which is used in the stationary energy storage. Simulation and experiment results prove its superior performance in accuracy compared with conventional methods.

Keywords: state of charge, battery management system, parameter identification, dual adaptive extended Kalman filter, stationary energy storage

1. INTRODUCTION

Electrochemical energy storage is getting more and more attention on renewable energy integration. Liquid metal battery (LMB) is a newly developed battery chemistry for stationary energy storage [1], which has a low material cost and a long cycle life [2]. To ensure the safe and reliable operation of these batteries applied in energy storage system (ESS), a battery management system (BMS) is necessarily developed. In BMS, SOC estimation is one of the most important functions.

A lot of literatures reported on the SOC estimation algorithms, which mainly can be divided into three categories, conventional methods, model-based methods and data-driven methods. Nowadays, model-based methods are widely used due to its simple implement and high accuracy, such as Kalman Filter , Extended Kalman Filter [3], Unscented Kalman Filter [4], Particle Filter [5], H-infinity Filter [6], Sliding Mode Observer [7] and so on. Adaptive Kalman methods are also studied before, including adaptive extended Kalman filter, adaptive unscented Kalman Filter [8], et al. In addition, state and parameter co-estimation is also reported in literatures, including dual and joint methods [10]-[13].

In this paper, a novel dual adaptive extended Kalman filter is proposed, which estimates the battery states and parameters at the same time. Moreover, the adaptive method adjusts the process and measurement noise covariances in the SOC estimation process, improving the robustness of the algorithm. Compared with EKF and AEKF, it can achieve higher accuracy.

2. BATTERY MODEL

From the electrochemical impedance spectroscopy of liquid metal battery, two different time constants can be extracted [9]. On this basis, a second order Thevenin equivalent circuit model is utilized to describe the behavior of LMB as shown in Fig. 1. It consists of a controlled voltage source $U_{oc}(z)$, an ohmic resistance R_s and two RC circuits.

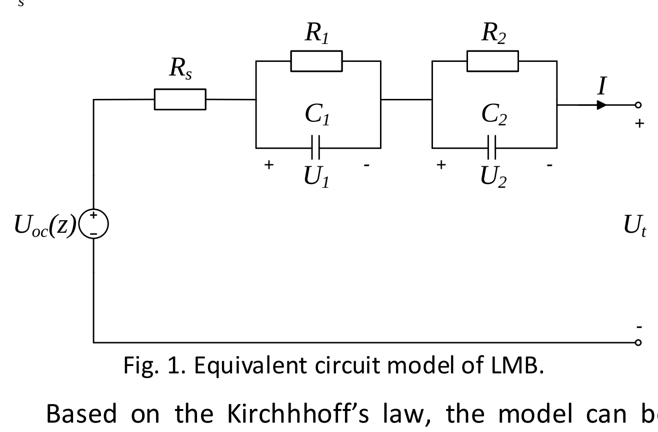

Fig. 1. Equivalent circuit model of LMB.

Based on the Kirchhhoff's law, the model can be expressed as:

$$
\begin{cases}
\dot{U}_1 = -\frac{1}{R_1 C_1} U_1 + \frac{1}{C_1} I \\
\dot{U}_2 = -\frac{1}{R_2 C_2} U_2 + \frac{1}{C_2} I \\
U_t = U_{oc}(z) - U_1 - U_2 - IR_s
\end{cases} \tag{1}
$$

where $U_{oc}(z)$ represents the open circuit voltage, which is a function of z. U_t is the terminal voltage, I is the load current and $U_i(i=1,2)$ is the polarization voltage. z denotes the SOC, which is formulated as

$$
z = z_0 - \int I(t)/C_n dt \tag{2}
$$

where z_0 represents the initial battery SOC and C_n denotes the maximum available capacity of the battery.

The discretization form of Eq.(1) is

$$
\begin{cases}
U_{1,k} = e^{-\Delta t/\tau_1} U_{1,k-1} + \left(1 - e^{-\Delta t/\tau_1}\right) I_{k-1} R_1 \\
U_{2,k} = e^{-\Delta t/\tau_2} U_{2,k-1} + \left(1 - e^{-\Delta t/\tau_2}\right) I_{k-1} R_2 \\
U_{t,k} = U_{oc}(z_k) - U_{1,k} - U_{2,k} - I_k R_s
\end{cases} \tag{3}
$$

where, k denotes the discretization step with a sample interval of Δt, $k = 1,2,3,\ldots,n$. $\tau_i = R_i C_i (i=1,2)$ and

$$
z_k = z_{k-1} - I_{k-1} \Delta t / C_n \tag{4}
$$

Defining $\alpha_i = \mathbf{exp}(-\Delta t/\tau_i)$ and combining Eq.(3) and (4), the battery state-space equation can be obtained as

$$
\begin{cases}
\begin{bmatrix} z_{k+1} \\ U_{1,k+1} \\ U_{2,k+1} \end{bmatrix} = \begin{bmatrix} 1 & 0 & 0 \\ 0 & \alpha_1 & 0 \\ 0 & 0 & \alpha_2 \end{bmatrix} \begin{bmatrix} z_k \\ U_{1,k} \\ U_{2,k} \end{bmatrix} + \begin{bmatrix} -\Delta t/C_n \\ (1-\alpha_1) R_1 \\ (1-\alpha_2) R_2 \end{bmatrix} I_k + \boldsymbol{\omega}_k \\
U_{t,k} = U_{oc}(z_k) - U_{1,k} - U_{2,k} - I_k R_s + \upsilon_k
\end{cases} \tag{5}
$$

where $\boldsymbol{\omega}_k$ and υ_k represent the process noise and the measurement noise, respectively.

Define the model parameters vector as

$$
\boldsymbol{\theta} = \begin{bmatrix} R_s & \alpha_1 & \alpha_2 & R_1 & R_2 \end{bmatrix} \tag{6}
$$

Due to battery parameters change slowly over time, they can be treated as constant with some small perturbation. Thus, the battery parameters state-space equation can be achieved by

$$
\begin{cases}
\boldsymbol{\theta}_{k+1} = \boldsymbol{\theta}_k + \boldsymbol{r}_k \\
U_{t,k} = U_{oc}(z_k) - U_{1,k} - U_{2,k} - I_k R_s + e_k
\end{cases} \tag{7}
$$

where $\boldsymbol{r}_k$ denotes a fictitious input to model the slow drift in the parameter values of the battery and e_k models the sensor noise and modeling error.

3. DUAL ADAPTIVE EXTENDED KALMAN FILTER

In order to improve the accuracy and robustness of SOC estimation algorithm, state and parameter co-estimation is widely used. However, the joint estimation method augment the model state vector with model parameters, which results in high-dimensional matrix operations. In additon, conventional filters suffer from unknown noise characteristics of the system. Therefore, the dual adaptive extended Kalman filter proposed here uses two seperate AEKF for state estimation and parameter estimation, respectively.

For the sake of simplicity, rewrite Eq.(5) and Eq.(7) in a general form as follows, respectively.

$$
\begin{cases}
\boldsymbol{x}_{k+1} = f(\boldsymbol{x}_k, u_k, \boldsymbol{\theta}_k) + \boldsymbol{\omega}_k \\
y_k = h(\boldsymbol{x}_k, u_k, \boldsymbol{\theta}_k) + \upsilon_k
\end{cases} \tag{8}
$$

$$
\begin{cases}
\boldsymbol{\theta}_{k+1} = \boldsymbol{\theta}_k + \boldsymbol{r}_k \\
d_k = g(\boldsymbol{x}_k, u_k, \boldsymbol{\theta}_k) + e_k
\end{cases} \tag{9}
$$

where $\boldsymbol{x}_k = \begin{bmatrix} z_k & U_{1,k} & U_{2,k} \end{bmatrix}^T$ and $u_k = I_k$. $f(\bullet)$ is the state transition function. y_k is equal to d_k, which both represent the battery terminal voltage. $h(\bullet)$ is equal to $g(\bullet)$, which both denote the measurement function.

Based on the nonlinear state-space equtions, the relevant matrixes for the dual AEKF estimator can be calculated as,

$$
\begin{cases}
\boldsymbol{A}_k = \frac{\partial f(\boldsymbol{x}_k, u_k, \boldsymbol{\theta}_k^-)}{\partial \boldsymbol{x}_k}\Big|_{\boldsymbol{x}_k = \hat{\boldsymbol{x}}_k^+} = \begin{bmatrix} 1 & 0 & 0 \\ 0 & \alpha_1 & 0 \\ 0 & 0 & \alpha_2 \end{bmatrix} \\
\boldsymbol{C}_k^x = \frac{\partial h(\boldsymbol{x}_k, u_k, \boldsymbol{\theta}_k^-)}{\partial \boldsymbol{x}_k}\Big|_{\boldsymbol{x}_k = \hat{\boldsymbol{x}}_k^-} = \begin{bmatrix} \frac{\partial U_{oc}}{\partial z}\Big|_{z=z_k} & -1 & -1 \end{bmatrix}^T \\
\boldsymbol{C}_k^\theta = \frac{dg(\hat{\boldsymbol{x}}_k^-, u_k, \boldsymbol{\theta})}{d\boldsymbol{\theta}}\Big|_{\boldsymbol{\theta} = \hat{\boldsymbol{\theta}}_k^-}
\end{cases} \tag{10}
$$

where the calculation of C_k^θ requires a total differential expansion,

$$
\frac{dg(\hat{\boldsymbol{x}}_k^-, u_k, \boldsymbol{\theta})}{d\boldsymbol{\theta}} = \frac{\partial g(\hat{\boldsymbol{x}}_k^-, u_k, \boldsymbol{\theta})}{\partial \boldsymbol{\theta}} + \frac{\partial g(\hat{\boldsymbol{x}}_k^-, u_k, \boldsymbol{\theta})}{\partial \hat{\boldsymbol{x}}_k^-} \frac{d\hat{\boldsymbol{x}}_k^-}{d\boldsymbol{\theta}} \tag{11}
$$

$$
\frac{d\hat{\boldsymbol{x}}_k^-}{d\boldsymbol{\theta}} = \frac{\partial f(\hat{\boldsymbol{x}}_{k-1}^+, u_{k-1}, \boldsymbol{\theta})}{\partial \boldsymbol{\theta}} + \frac{\partial f(\hat{\boldsymbol{x}}_{k-1}^+, u_{k-1}, \boldsymbol{\theta})}{\partial \hat{\boldsymbol{x}}_{k-1}^+} \frac{d\hat{\boldsymbol{x}}_{k-1}^+}{d\boldsymbol{\theta}} \tag{12}
$$

$$
\frac{d\hat{\boldsymbol{x}}_{k-1}^+}{d\boldsymbol{\theta}} = \frac{d\hat{\boldsymbol{x}}_{k-1}^-}{d\boldsymbol{\theta}} - \boldsymbol{L}_{k-1}^x \frac{dg(\hat{\boldsymbol{x}}_{k-1}^-, u_{k-1}, \boldsymbol{\theta})}{d\boldsymbol{\theta}} \tag{13}
$$

where $\boldsymbol{L}_{k-1}^x$ is the Kalman gain for the state filter, which is assumed not to be a function of θ.

The three derivatives $dg/d\boldsymbol{\theta}$, $d\hat{\boldsymbol{x}}_k^-/d\boldsymbol{\theta}$ and $d\hat{\boldsymbol{x}}_{k-1}^+/d\boldsymbol{\theta}$ are initialized to be zero and computed recursively as the filters operate.The specific algorithm is described as follows:

1) Initialization

$$
\hat{\boldsymbol{\theta}}_0^+ = E[\boldsymbol{\theta}_0], \Sigma_{\boldsymbol{\theta},0}^+ = E\left[\left(\boldsymbol{\theta}_0 - \hat{\boldsymbol{\theta}}_0^+\right)\left(\boldsymbol{\theta}_0 - \hat{\boldsymbol{\theta}}_0^+\right)^T\right] \tag{14}
$$

$$
\hat{\boldsymbol{x}}_0^+ = E[\boldsymbol{x}_0], \Sigma_{\boldsymbol{\theta},0}^+ = E\left[\left(\boldsymbol{x}_0 - \hat{\boldsymbol{x}}_0^+\right)\left(\boldsymbol{x}_0 - \hat{\boldsymbol{x}}_0^+\right)^T\right] \tag{15}
$$

2) Parameter filter time update

$$\hat{\boldsymbol{\theta}}_k^- = \hat{\boldsymbol{\theta}}_{k-1}^+ \tag{16}$$

$$\Sigma_{\theta,k}^- = \Sigma_{\theta,k-1}^- + \Sigma_r \tag{17}$$

3) State filter time update

$$\hat{\boldsymbol{x}}_k^- = f\left(\hat{\boldsymbol{x}}_{k-1}^+, u_{k-1}, \hat{\boldsymbol{\theta}}_k^-\right) \tag{18}$$

$$\Sigma_{x,k}^- = \boldsymbol{A}_{k-1}\Sigma_{x,k-1}^+ \boldsymbol{A}_{k-1}^T + \Sigma_\omega \tag{19}$$

4) State filter measurement update

$$\boldsymbol{L}_k^x = \Sigma_{x,k}^- \left(\boldsymbol{C}_k^x\right)^T \left[\boldsymbol{C}_k^x \Sigma_{x,k}^- \left(\boldsymbol{C}_k^x\right)^T + \Sigma_\upsilon\right]^{-1} \tag{20}$$

$$\hat{\boldsymbol{x}}_k^+ = \hat{\boldsymbol{x}}_k^- + \boldsymbol{L}_k^x \left[y_k - h\left(\hat{\boldsymbol{x}}_k^-, u_k, \hat{\boldsymbol{\theta}}_k^-\right)\right] \tag{21}$$

$$\Sigma_{x,k}^+ = \left(\boldsymbol{I} - \boldsymbol{L}_k^x \boldsymbol{C}_k^x\right)\Sigma_{x,k}^- \tag{22}$$

5) Parameter filter measurement update

$$\boldsymbol{L}_k^\theta = \Sigma_{\theta,k}^- \left(\boldsymbol{C}_k^\theta\right)^T \left[\boldsymbol{C}_k^\theta \Sigma_{\theta,k}^- \left(\boldsymbol{C}_k^\theta\right)^T + \Sigma_e\right]^{-1} \tag{23}$$

$$\hat{\boldsymbol{\theta}}_k^+ = \hat{\boldsymbol{\theta}}_k^- + \boldsymbol{L}_k^\theta \left[d_k - g\left(\hat{\boldsymbol{x}}_k^-, u_k, \hat{\boldsymbol{\theta}}_k^-\right)\right] \tag{24}$$

$$\Sigma_{\theta,k}^+ = \left(\boldsymbol{I} - \boldsymbol{L}_k^\theta \boldsymbol{C}_k^\theta\right)\Sigma_{\theta,k}^- \tag{25}$$

6) Adjustment process

$$\varepsilon_k = y_k - h\left(\hat{\boldsymbol{x}}_k^+, u_k, \hat{\boldsymbol{\theta}}_k^+\right) \tag{26}$$

$$c_k = \frac{1}{L}\sum_{i=k-L+1}^{k} \varepsilon_i \varepsilon_i^T \tag{27}$$

$$\begin{cases} \Sigma_\omega = \boldsymbol{L}_k^x c_k \left(\boldsymbol{L}_k^x\right)^T, \quad \Sigma_\upsilon = c_k + \boldsymbol{C}_k^x \Sigma_{x,k}^+ \left(\boldsymbol{C}_k^x\right)^T \\ \Sigma_r = \boldsymbol{L}_k^\theta c_k \left(\boldsymbol{L}_k^\theta\right)^T, \quad \Sigma_e = c_k + \boldsymbol{C}_k^\theta \Sigma_{\theta,k}^+ \left(\boldsymbol{C}_k^\theta\right)^T \end{cases} \tag{28}$$

where L is the size of the moving average window.

4. RESULTS AND DISCUSSIONS

To varify the accuracy of the proposed dual AEKF, a lab-made LMB was tested under Federal Urban Driving Schedules (FUDS). The design capacity of the tested LMB is 23 Ah and its nominal voltage/current are 0.8 V/ 0.2 C.

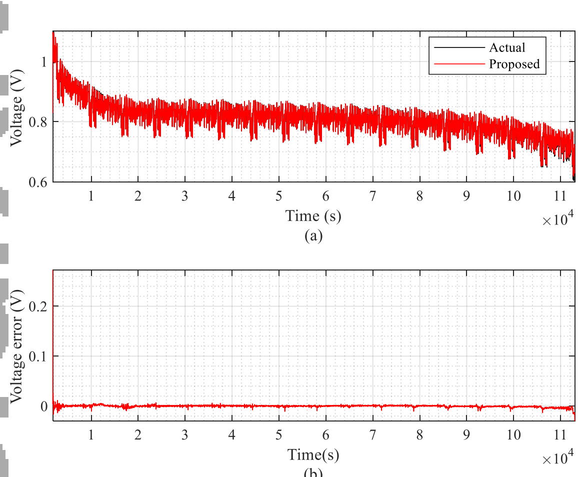

Fig. 2. Voltage prediction results: (a) predicted terminal voltage; (b) terminal voltage prediction error.

The cut-off voltage is 1.2 V/0.6 V. Arbin BT2000 tester is used for battery test and the sampling frequency is 1 Hz.

The battery was fully charged under constant current constant voltage (CCCV). Then the FUDS profiles were loaded to discharge the battery. Both battery voltage and current are recorded for further simulation.

The initial SOC is set to be 0.5 and the polarization voltage are both set to be 0. The initial parameters use the offline identification results as the best guess.

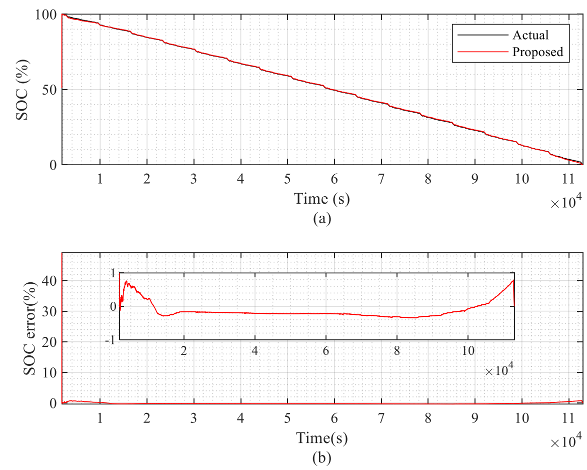

Fig. 3. SOC estimation results: (a) SOC; (b) SOC error.

Moreover, to prove the robustness of the proposed algorithm, a 5 mV Guassian noise is added to the voltage measurement and a 1 mA Guassian noise is added to the current measurement.

The battery terminal voltage prediction results are shown in Fig. 2. As illustrated in Fig. 2(a), the predicted voltage curve is almost coincided with the measured voltage curve. The maximum voltage prediction error is less than 0.005 mV as seen in Fig. 2(b).

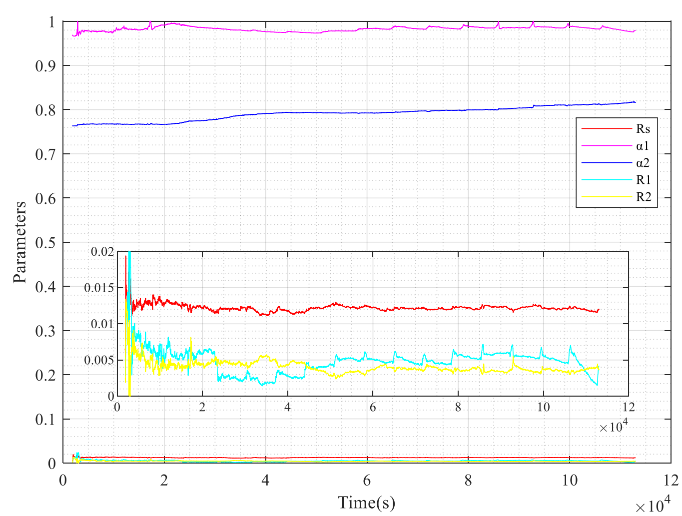

Fig. 4. Estimation results of model parameters.

The SOC estimation results are depicted in Fig. 3. It can be seen that the maximum SOC estimation error is less than 0.5% except the start and end of discharging. Drastic changes in parameters may be the reason for the larger estimation error in paticular working range, which is illustrated in Fig. 4.

As shown in Fig. 4, model paramets change drasticlly at the start of discharging. It can be caused by the erroneous initials. At the end of discharging, the battery polarization resistance R_2 also has a obvious change.

Fig. 5 gives the SOC estimation results using different initial SOC settings. It proves that the inital value has no influence on the convergence of the proposed algorithm. Nevertheless, when the inital SOC is closer to the actual value, the algorithm will have a faster convergence rate and a higher accuracy.

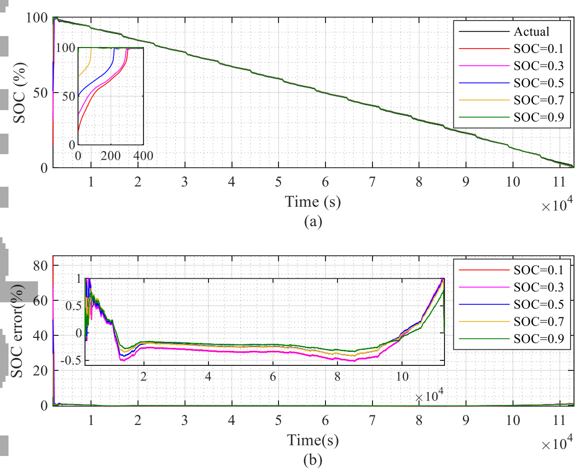

Fig. 5. Comparison results of SOC estimation using different initial SOCs: (a) SOC; (b) SOC error.

The performance of the proposed dual AEKF is also compared with conventional methods as shown in Fig. 6.

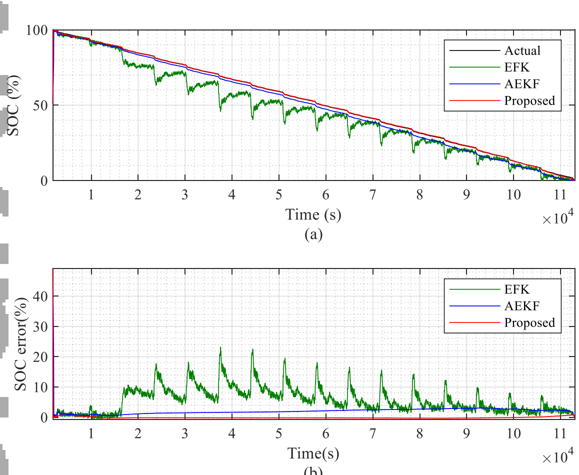

Fig. 6. Comparison results of SOC estimation using different methods (initial SOC=0.5): (a) SOC; (b) SOC error.

EKF achieves the worst performance due to its fixed model parameters and non-adaptive noise covariance. Although AEKF also use fixed model parameters, it shows a much better performance because of its adaptive noise covariance. Compared with EKF and AEKF, the proposed dual AEKF exhibits superior performance in estimation accuracy. The maximum SOC estimation error of EKF is more than 20% and that of AEKF is more than 5%, while the maximun SOC estimation error of proposed dual AEFK is less than 1%. It indicates that real-time parameter identification and adaptive noise covariance are of significant importance to the SOC estimation.

5. CONCLUSIONS

A dual AEKF has been proposed for the online SOC and parameter co-estimation of LMBs. Compared with the joint method, the proposed algorithm avoids high-dimensional matrix operations. Meanwhile, the adaptive noise covariances and real-time parameter identification in the estimation process improve the robustness of the algorithm. The proposed algorithm can converge quickly with any erroneous initial values. Under FUDS test profiles, the maximum SOC estimation error of the proposed algorithm is less than 1% while EKF is more than 20% and AEKF is more than 5%.

ACKNOWLEDGEMENT

This work is supported by the National Key Research and Development Program of China (2018YFB0905600) and the National Natural Science Foundation of China (Grant No. U1766216).

REFERENCES

[1] Wang K, Jiang K, Chung B, Ouchi T, Burke PJ, Boysen DA, et al. Lithium–antimony–lead liquid metal battery for grid-level energy storage. Nature. 2014; 514:348.

[2] Li H, Wang K, Cheng S, Jiang K. High Performance Liquid Metal Battery with Environmentally Friendly Antimony–Tin Positive Electrode. ACS Applied Materials & Interfaces. 2016; 8:12830-5.

[3] Plett GL. Extended Kalman filtering for battery management systems of LiPB-based HEV battery packs: Part 3. State and parameter estimation. Journal of Power Sources. 2004; 134:277-92.

[4] Plett GL. Sigma-point Kalman filtering for battery management systems of LiPB-based HEV battery packs: Part 1: Introduction and state estimation. Journal of Power Sources. 2006; 161:1356-68.

[5] Tulsyan A, Tsai Y, Gopaluni RB, Braatz RD. State-of-charge estimation in lithium-ion batteries: A particle filter approach. Journal of Power Sources. 2016; 331:208-23.

[6] Lin C, Mu H, Xiong R, Shen W. A novel multi-model probability battery state of charge estimation approach for electric vehicles using H-infinity algorithm. Applied Energy. 2016; 166:76-83.
[7] Kim IS. The novel state of charge estimation method for lithium battery using sliding mode observer. Journal of Power Sources. 2006; 163:584-90.
[8] Sun F, Hu X, Zou Y, Li S. Adaptive unscented Kalman filtering for state of charge estimation of a lithium-ion battery for electric vehicles. Energy. 2011; 36:3531-40.
[9] Xu, C, Cheng S, Wang K, & Jiang K. A Fractional-order Model for Liquid Metal Batteries. Energy Procedia. 2019; 158:4690-4695.
[10] Liu G, Xu C, Li H, Jiang K, Wang K. State of charge and online model parameters co-estimation for liquid metal batteries. Applied Energy. 2019;250:677-84.
[11] Dong G, Wei J, Zhang C, Chen Z. Online state of charge estimation and open circuit voltage hysteresis modeling of LiFePO4 battery using invariant imbedding method. Applied Energy. 2016; 162:163-71.
[12] Cai M, Chen W, Tan X. Battery state-of-charge estimation based on a dual unscented Kalman filter and fractional variable-order model. Energies. 2017; 10:1577.
[13] Plett GL. Battery management systems, Volume II: Equivalent-circuit methods. Artech House; 2015.